



Hybrid tin oxide-SWNT nanostructures based gas sensor

Syed Mubeen^a, Min Lai^b, Ting Zhang^c, Jae-Hong Lim^a, Ashok Mulchandani^a, Marc A. Deshusses^d, Nosang V. Myung^{a,*}

^a Department of Chemical and Environmental Engineering, University of California – Riverside, Riverside, CA 92521, United States

^b School of Mathematics and Physics, Nanjing University of Information Science & Technology, Nanjing 210044, People's Republic of China

^c Suzhou Institute of Nano-tech and Nano-bionics (SINANO), Chinese Academy of Science (CAS), Suzhou 215125, People's Republic of China

^d Department of Civil and Environmental Engineering, Duke University, Durham, NC 27708, United States

ARTICLE INFO

Article history:

Received 27 September 2012

Received in revised form 9 November 2012

Accepted 5 January 2013

Available online 11 January 2013

Keywords:

Single-walled carbon nanotube

Tin oxide

Gas sensor

Electrochemical deposition

Chemiresistor

Field effect transistor

ABSTRACT

A facile electrochemical functionalization method was utilized to decorate single-walled carbon nanotubes (SWNTs) with tin oxide and their gas sensing performance toward various analytes (NH₃, NO₂, H₂, H₂S, acetone, and water vapor) was evaluated at room temperature. Tin oxy-hydroxide was site-specifically precipitated on the surface of SWNTs because of an increase in local pH during electrochemical reduction of nitrate to nitrite ions. By adjusting the amount of charge passed during deposition, the amount of tin oxide deposited on SWNTs was controlled, which altered the electronic and gas sensing properties of the nanostructures. The resulting hybrid nanostructures showed excellent sensitivities upon exposure to trace amounts of both oxidizing gases (limit of detection (LOD) of 25 ppbv for NO₂) and reducing gases (LOD of 10 ppmv for H₂) at room temperature. The enhanced sensing performance was due to the charge transfer between the surface active tin oxide nanoparticles and SWNTs, with the direction of charge transfer depending on the analyte gas. This approach can be applied to fabricate other hybrid metal oxide-SWNTs nanostructures to create highly sensitive gas sensor arrays.

© 2013 Elsevier Ltd. All rights reserved.

1. Introduction

Interaction between metal oxide surface and surrounding gas has been known and extensively studied. Indeed, most of commercial solid-state chemical sensors are based on thick/thin film of doped metal oxides (e.g., SnO₂, In₂O₃, and ZnO doped with platinum, palladium, etc.) [1,2]. The operating principle of these sensors is based on the surface interaction between metal oxide and analyte. Under ambient conditions, oxygen vacancies are formed on the metal oxide surface due to chemisorption of oxygen, which later exchange electrons with the bulk of material resulting in the formation of an electronic depletion layer close to the surface (i.e., surface charge layer) [3,4]. Thus, when a reducing gas (e.g., CO, H₂, and NH₃) comes in contact with the metal oxide surface, it reacts with surface oxygen, which then leads to injection of electrons, into nanostructures. It has been observed that when the grain size is comparable to the Debye length, a space charge region is formed in the entire crystallite [4]. Hence significant improvements in gas sensing performance can be achieved by reducing the dimension of nanostructures down to the thickness of Debye length.

Several methods have been employed to synthesize metal oxide nanostructures with different morphologies including nanoparticles [5], nanowires [6], nanobelts [7], nanotubes [8], etc. Most of the initial demonstrations on metal oxide nano-gas sensors have been based on tin oxide (SnO₂) nanowires [9–11]. SnO₂ is a wide band gap ($E_g = 3.6$ eV at 300 K) n-type semiconductor, with excellent mechanical stability making it a suitable candidate for gas sensors. Although, a few works report utilizing metal oxide nano-gas sensor for rapid and sensitive detection of analytes, most of these sensors need to be operated at high temperatures due to their poor electrical conductivity at near room temperature which led to high power consumption [12,13]. To provide favorable electronic conduction pathways at room temperature while maintaining its excellent molecular recognition capability, major efforts have been made toward creating hybrid nanostructures [14–18]. Various methods were utilized to synthesize these hybrid nanostructures including sputtering [14], hydrothermal synthesis [15], electrospinning [16], chemical synthesis [17], etc. While the hybrid nanostructures synthesized with these methods demonstrated promising applications toward gas sensing, these methods are expensive, have poor selectivity for the template or lack of control over the amount of deposited materials. In addition, there are some inconsistencies observed over the sensing performance of such hybrid nanostructures, with resistance decreasing for both oxidizing and reducing gas species [14,16,18].

* Corresponding author.

E-mail address: myung@engr.ucr.edu (N.V. Myung).

Electrochemically assisted deposition has been successfully used to synthesize metal oxide thin films and nanostructures like SnO_2 [8], TiO_2 [19], and SiO_2 [20], etc. by increasing locally the solution pH, which leads to chemical precipitation of metal oxide or oxyhydroxide. Herein, we report a simple, efficient, controllable, electrochemical functionalization of single-walled carbon nanotubes (SWNTs) with tin oxide nanoparticles. Electrochemical quartz crystal microbalance (EQCM) and other electroanalytical techniques were utilized to investigate the effect of various electrochemical parameters including electrolyte composition, applied deposition potential, deposition rate, and morphology. By adjusting the amount of SnO_2 deposited on SWNTs, the sensing performance was optimized. Electrochemically functionalized SnO_2 on SWNTs surpass the earlier attempted approaches, while still addressing all the requirements typical for a gas sensor including inexpensive synthesis approach, room temperature operation, sensitive detection, etc.

2. Experimental

2.1. AC dielectrophoretic (DEP) alignment of SWNTs across microfabricated gold electrodes

A single walled carbon nanotubes suspension was prepared by addition of 0.2 mg of commercially available carboxylated SWNTs (Carbon Solutions Inc., Riverside, CA) to 20 mL of N,N-dimethylmethanamide (DMF). The contents were sonicated in a glass vial for 90 min using a VWR model 50D sonicator. All 20 mL of the SWNT suspension were transferred to a 50 mL Teflon centrifuge tube and centrifuged for 90 min at $15,000 \times g$ and 23°C using a Beckman J2-HS centrifuge. Immediately after centrifugation, 10 mL of the supernatant was carefully removed and placed in a glass vial. The supernatant was sonicated for an additional 60 min prior to use. Lithographically patterned Si chips with 16 gold electrode pairs (Ti/Au 20/180 nm thick layers) were utilized as substrates and contacts for sensor assemblages (Fig. S1). The electrodes contained a $3 \times 200 \mu\text{m}$ gap and large contact pads that enabled individual addressability for electrochemical functionalization [21]. SWNTs were aligned across the electrode gaps via AC DEP alignment by adding 1.5 μL drop of SWNT suspension, and applying 1 V (peak to peak) and 4 MHz (Keithley 3390 AC generator, 50 MHz arbitrary waveform generator) frequency. The device resistance was controlled by the alignment time [21]. After nanotube alignment, the nanostructures were annealed for 1 h at 300°C under a reducing environment (5% H_2 + 95% N_2) to minimize the contact resistance between the nanotubes and electrode pads.

2.2. Electrochemical assisted deposition of tin oxide

Two different electrolytes were utilized for SnO_2 deposition on SWNTs. Solution A consisted of 100 mM NaNO_3 ($\geq 99.0\%$, Sigma–Aldrich, MO), 75 mM of HNO_3 (70%, Sigma–Aldrich, MO), and 20 mM of $\text{SnCl}_2 \cdot 5\text{H}_2\text{O}$ ($\geq 98\%$, Sigma–Aldrich, MO) [8]. Solution B consisted of 20 mM of $\text{SnCl}_2 \cdot 5\text{H}_2\text{O}$ in the absence of nitrate. The pH of both the solutions was adjusted to 1.3 by adding concentrated HCl (37%, Sigma–Aldrich, MO), and the solutions were aged for 12 h. Two different working electrodes were used throughout the experiment. For electrochemical quartz crystal microbalance (EQCM) studies, spray-printed SWNTs on gold coated quartz-crystal resonators (type 1) were used as the working electrode which was immersed in 10 mL of electrolyte with the Pt counter (99.99%, Sigma–Aldrich, MO) and the Ag/AgCl reference electrodes fabricated in our laboratory to form electrochemical cell. For electrical characterization and sensing experiments, AC DEP aligned SWNTs between two gold electrodes (type 2) were used as the working

electrode. The electrochemical cell was formed by dispensing a 3 μL drop of electrolyte on top of the aligned SWNTs network and positioning platinum and Ag/AgCl wires inside the droplet using micropositioners. Linear sweep voltammetry (LSV) and chronoamperometry (CA) were carried out at room temperature using a potentiostat/galvanostat (EG&G, Princeton Applied Research 263A Potentiostat/Galvanostat, NY). During LSV experiment, the potentials were scanned from +100 mV of open circuit potential to -1.0 V vs. Ag/AgCl at a scan rate of 10 mV s^{-1} . In situ monitoring of the deposition process during potential sweep was done using EQCM (Maxtek RQCM quartz microbalance instrument (INFICON, NY)). For CA experiments, a fixed cathodic potential (-0.4 V for solution A and -0.6 V for solution B vs. reference electrode) was applied for a defined period of time. After electrochemical assisted deposition, the working electrodes were immediately rinsed with deionized water to prevent any undesirable chemical precipitation. For materials characterization including XRD and FT-IR, tin oxide coated spray-printed SWNTs were used. For composition and morphology analysis (i.e., SEM, TEM, and EDX), tin oxide coated on AC DEP aligned SWNTs were used. Selected area electron diffraction (SAED) and EDX spectra were taken at random points.

2.3. Electrical characterization and gas sensing measurements

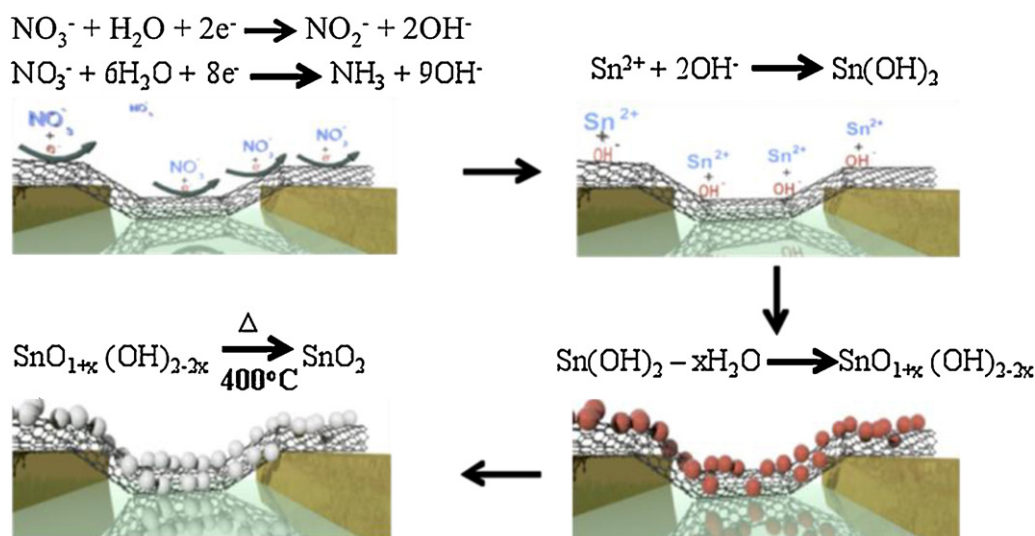
Electrical characterizations were performed in a three point probe configuration using Keithley 2636 System. The FET transfer characteristics were measured by applying a constant bias (V_{SD}) of 1 V between source and drain electrodes while sweeping gate voltages (V_{G}) between ± 20 V. For gas sensing studies, the functionalized chip was assembled onto a pin chip holder by wire bonding (West Bond Inc., Model 7443A) and was subsequently loaded on a custom made bread board designed for the sensing system [22]. Each sensor was subjected to 1.0 V DC potential and the current was continuously monitored, the electrical resistance was then determined by applying Ohm's Law. A baseline was achieved with exposure to dry air as the carrier gas (99.99% purity) and various analytes were tested by placing analyte cylinders in series to the dry air. Different analyte concentrations were attained by dilutions with the carrier gas. The exposure and recovery time was fixed at 15 and 20 min, respectively, while the gas flow rate was kept constant at 200 sccm by mass flow controllers (Alicat Scientific Incorporated) [21,22]. All experiments were performed at room temperature. All results shown in Figs. 5 and S2 are from 5 sensors or more, with resistance values selected in the range of 10–100 k Ω for consistency.

3. Results and discussion

3.1. Electroanalytical studies of SnO_2 on SWNTs

Scheme 1 illustrates the electrochemical functionalization of SWNTs with tin oxides. Unlike other methods, electrochemical functionalization with SnO_2 is simple, rapid and requires no pre-treatment of the substrate. It involves electrochemical reduction of nitrate ions by applying suitable cathodic potential to electrode (SWNTs in this case) resulting in the generation of hydroxyl ions. The generated hydroxyl ions then locally increase the pH near the electrode surface, resulting in the chemical precipitation of tin oxyhydroxide, which is later converted to tin oxide by annealing in nitrogen environment [8,19].

Various electroanalytical techniques including linear sweep voltammogram (LSV) and electrochemical quartz crystal microbalance (EQCM) were carried out at room temperature using a three electrode electrochemical cell configuration to determine the deposition mechanism and optimum deposition potential (see Section 2 for further details). Fig. 1 shows plots of LSVs and in situ



Scheme 1. Schematic representation of electrochemical assisted deposition of tin oxide on SWNTs.

EQCM (as mass deposits on the electrode, frequency drops) studies. As shown in the figure, the deposition process in the presence and absence of nitrate ions were significantly different. In the presence of nitrate ions, an increase in cathodic current is accompanied

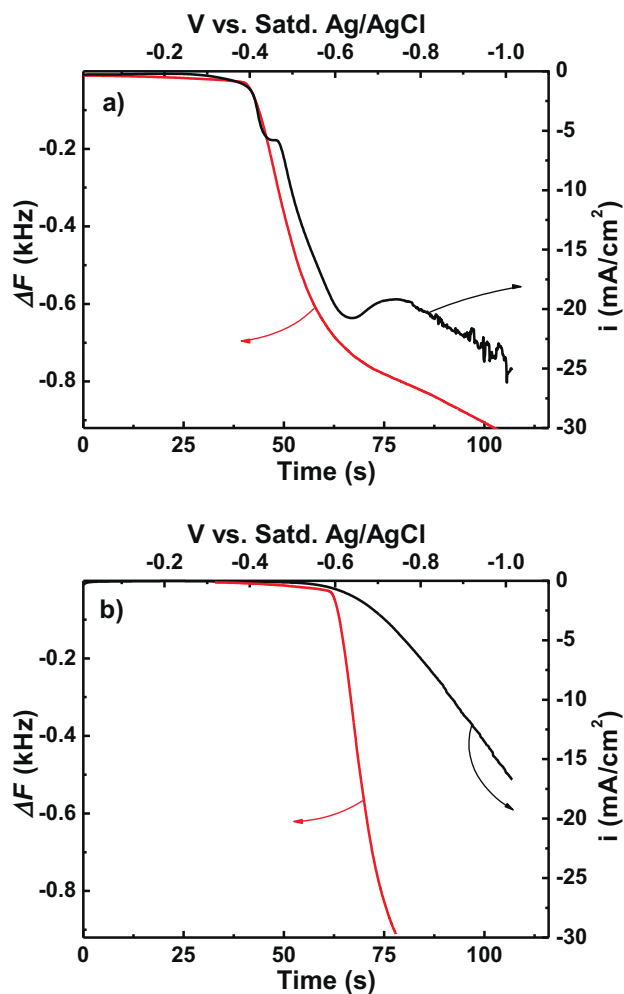


Fig. 1. Linear sweep voltammogram (LSV) and corresponding frequency–time plots for electrodeposition in the presence (a) and absence (b) of nitrate ions. The oscillation of current at negative potential ($E < -0.8\text{V}$) is due to hydrogen gas evolution.

by a simultaneous drop in frequency when the applied potential became more negative than -0.35V (Fig. 1a; all potentials referenced here are with respect to Ag/AgCl reference electrode). The cathodic peak observed in Fig. 1a was identified to be the electrochemical reduction of nitrate ions to nitrite ions or to ammonium ions. The corresponding increase in mass is attributed to the hydroxylation of tin precursor (due to local increase in pH) resulting in tin oxyhydroxide deposition on the substrate. In the case of solution B, cathodic current or frequency did not change until the applied potential became more negative than -0.6V (Fig. 1b). The sharp drop in frequency change observed for solution B at potentials more negative than -0.6V as confirmed through to metallic tin deposition. Both samples were then annealed in nitrogen atmosphere for 400°C for 4 h and were characterized using various techniques to determine their crystal structures and morphology.

3.2. Structural characterization

Fig. 2a shows XRD spectrum obtained using both solutions after annealing. Samples were potentiostatically deposited by applying -0.4V vs. Ag/AgCl for solution A and -0.6V vs. Ag/AgCl for solution B with a fixed deposition time of 5 min. Control sample was also fabricated by immersing working electrode (type 1) in solution A without applied potential for 5 min. The XRD spectrum of the deposit obtained from solution A (blue solid line, top trace) clearly shows the presence of tetragonal SnO_2 . XRD spectrum of the deposit from solution B (red solid line, center trace) shows the deposit contained metallic β -tin instead of SnO_2 consistent with the results of EQCM studies. The XRD spectrum for the control sample (black solid line, bottom trace) shows only diffraction peaks from substrate. FT-IR spectrum of SnO_2 coated SWNTs from solution A shows an absorption peak at 593cm^{-1} which corresponds to the vibration–absorption of Sn–O bond (Fig. 2b).

Fig. 3a and b shows a transmission electron microscopy (TEM) image of unfunctionalized and SnO_2 coated SWNT bundles, with corresponding high magnification images in the inset. The nanotubes appear mostly as bundles with very few individual nanotubes. Bundling may be due to the absence of ultra-high sonication step for TEM sample preparation leading to aggregation of SWNTs (see under methods for TEM sample preparation). As shown in Fig. 3b, TEM image shows the presence of isolated nanoparticles

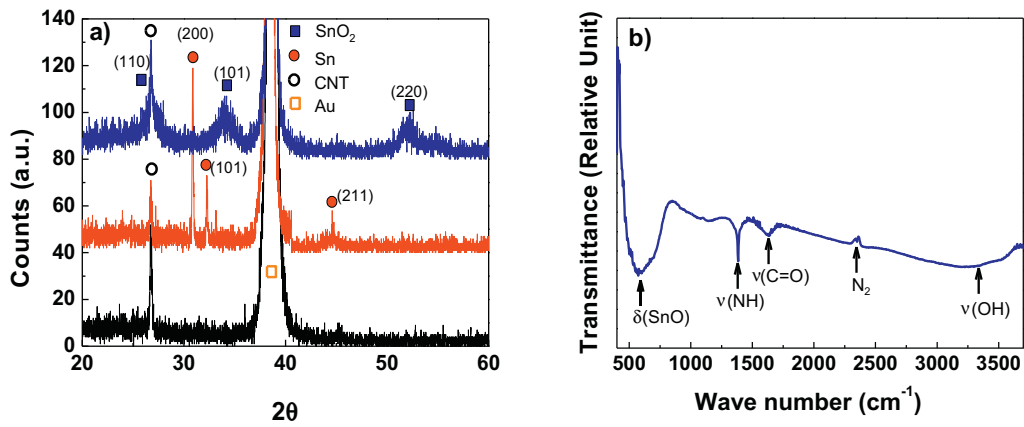


Fig. 2. (a) XRD spectrum of the products obtained using solution A (top, solid blue line), solution B (middle, red solid line) and control sample (bottom, black solid line). (b) FT-IR spectrum taken from KBr pellets containing SnO₂ coated SWNTs prepared using solution A at -0.4 V vs. Satd. Ag/AgCl for 5 min. (For interpretation of the references to color in this figure legend, the reader is referred to the web version of the article.)

on SWNTs after electrodeposition. Selected area electron diffraction (SAED) pattern (Fig. 3c) confirmed that the nanoparticles is polycrystalline tetragonal SnO₂ with (110), (101), (301) and (211) faces. EDX spectrum (Fig. 3d) of hybrid nanostructure shows the presence of Sn, O, and C which further confirms the presence of SnO₂ on SWNTs.

3.3. Electron transport and gas sensing properties

Fig. 4 shows field-effect transistor (FET) transport characteristics and scanning electron microscopy (SEM) images of SnO₂ coated SWNTs with different deposition charges using solution A at a constant deposition potential of -0.4 V vs. Ag/AgCl.

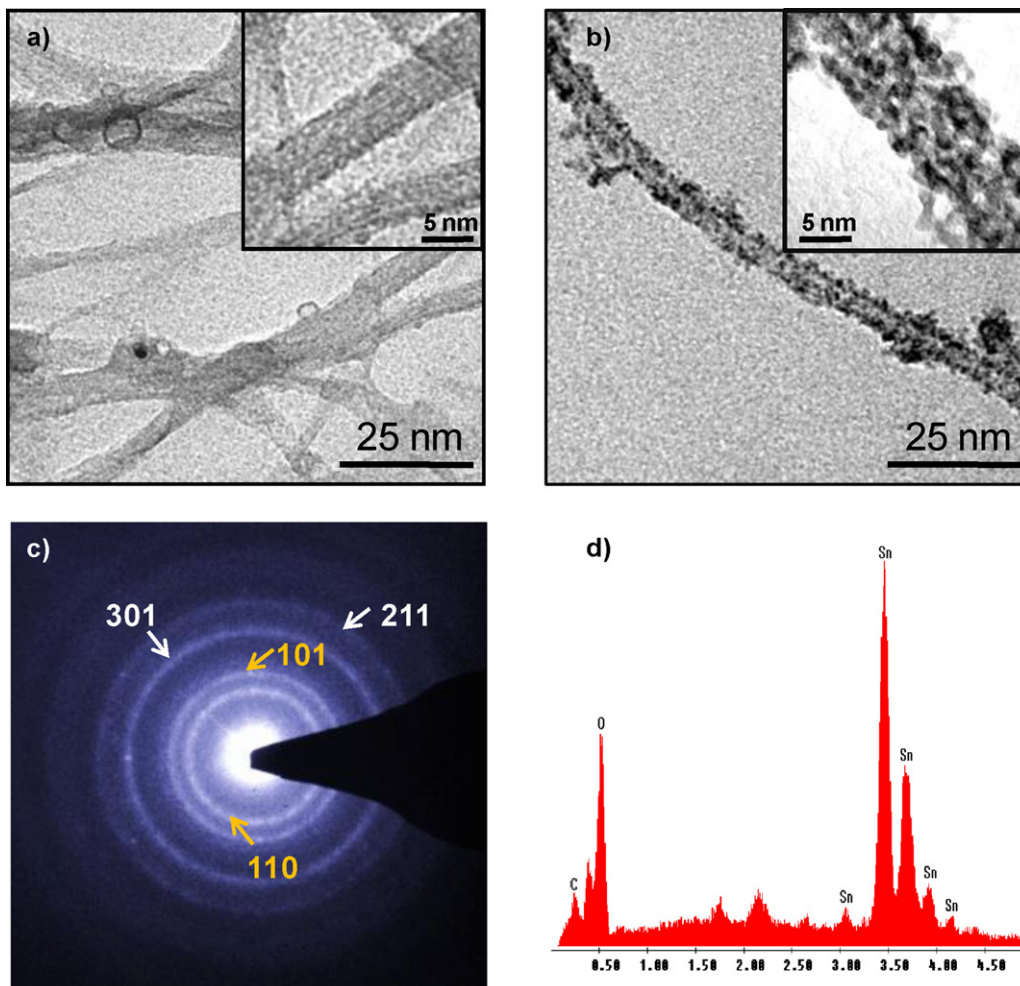


Fig. 3. TEM images of (a) bare SWNTs and (b) SWNTs coated with tin oxide (-0.4 V vs. Ag/AgCl wire, $5 \mu\text{C}$) with high magnification TEM image as the inset. (c) Selected area electron diffraction (SAED) pattern and (d) energy dispersive X-ray (EDX) spectrum collected from the SnO₂ coated SWNT sample.

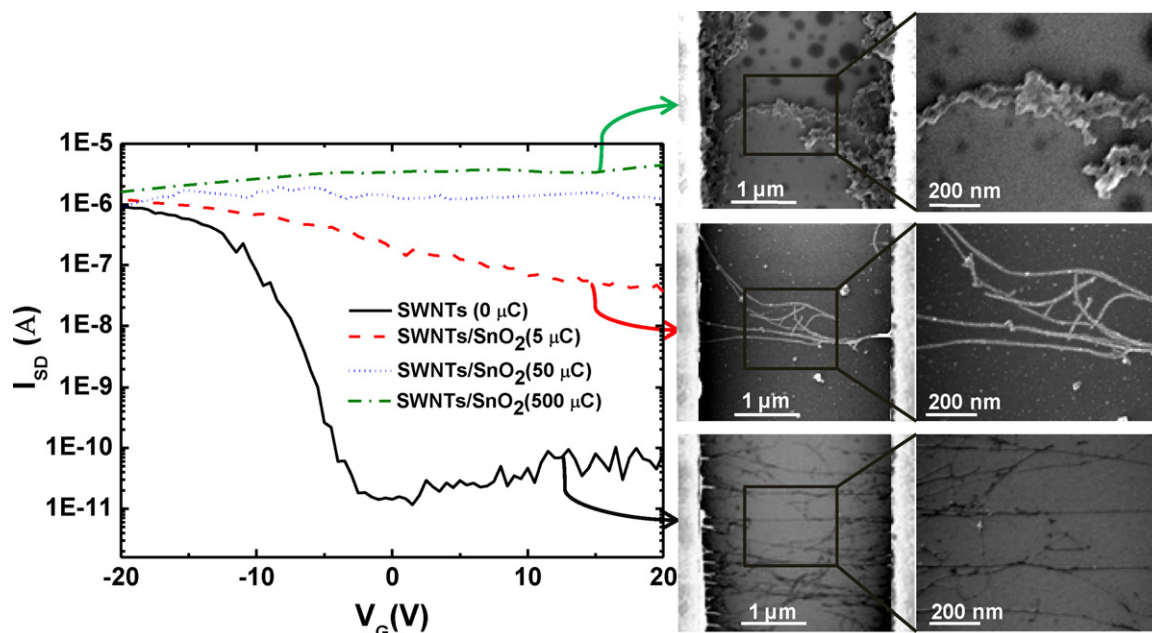


Fig. 4. FET transport characteristics and corresponding SEM images of SnO₂ coated SWNTs at different deposition charges. For the transfer measurements V_{SD} was fixed at 1 V. Highly doped silicon substrate was used as the back gate.

Two clear trends are noticeable. First and most obvious observation is the decrease in gate dependency with increasing deposition charge. Prior to deposition of SnO₂, the SWNT networks showed typical p-type behavior [23] in air with I_{on}/I_{off} ratio of around 10^5 . With increase in deposition charge, I_{on}/I_{off} ratio decreased to 10^2 to no gate dependency, to samples showing weak n-type behavior at high charge passed during deposition (i.e., 500 μ C). The decrease in gate dependency with deposition may be attributed to the introduction of more scattering sites, while the weak n-type

behavior observed at high deposition charge is due to the complete encapsulation of SWNTs with n-type SnO₂ resulting in a nanostructure in which the current is predominately passing through SnO₂ instead of SWNTs. The second obvious change is the increase in source–drain current after SnO₂ coating for all gate voltages which is due to increase in current channels (i.e., SnO₂ and SWNTs).

The introduction of SnO₂ nanocrystals, which are uniformly decorated along the surface of nanotubes, forms localized charge depletion regions at the SWNT–SnO₂ interface. If an oxidizing gas

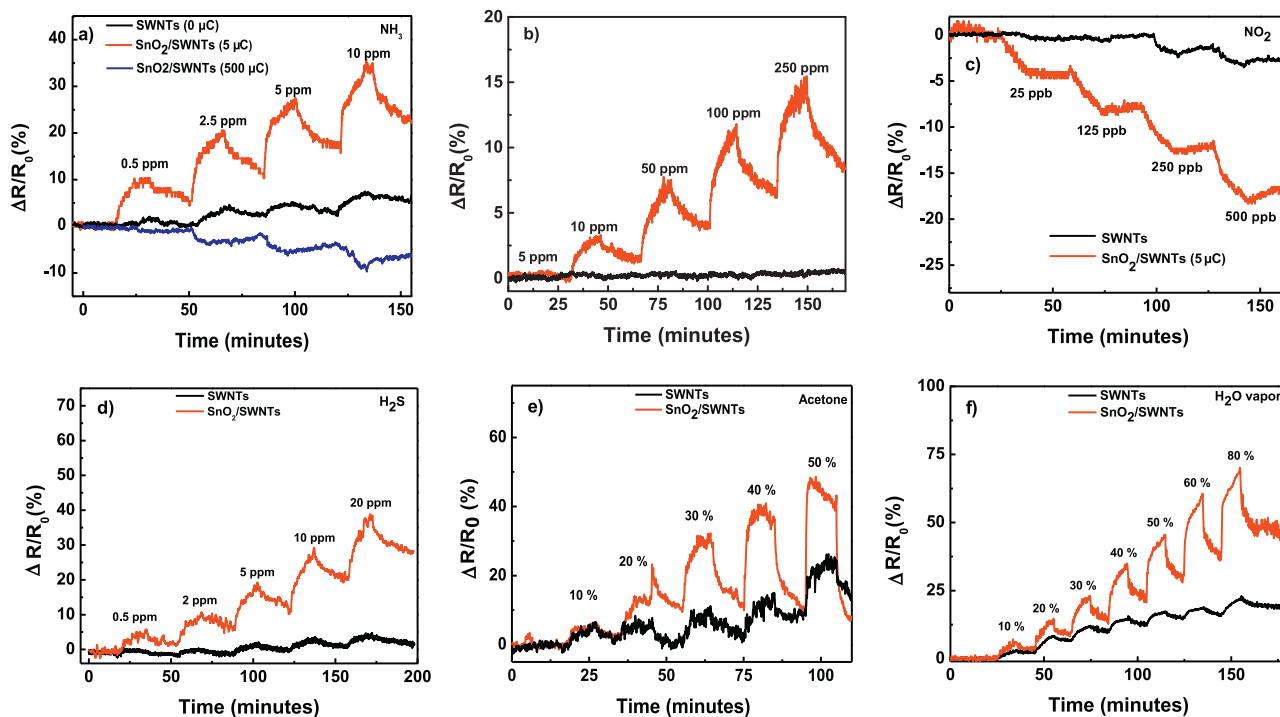


Fig. 5. Changes in resistance of unfunctionalized SWNT and SnO₂ coated SWNT sensor in air for different analytes: (a) NH₃, (b) H₂, (c) NO₂, (d) H₂S, (e) acetone, and (f) H₂O vapor. The deposition charge was varied from 0 μ C (black solid line) to 5 μ C (red solid line) to 500 μ C (solid blue line). (For interpretation of the references to color in this figure legend, the reader is referred to the web version of the article.)

Table 1

Comparison of LOD for SnO₂ nanowires (Refs. [9,27]), SnO₂ coated MWNTs (Ref. [14]), unfunctionalized SWNTs (this study) and SnO₂ coated SWNT (this study) toward NO₂ and H₂ at room temperature.

Analyte	SnO ₂ nanowires	MWNT–SnO ₂	Carboxylated SWNTs (this study)	SWNT–SnO ₂ (5 μC) (this study)
NO ₂	3 ppm [9]	25 ppm [14]	500 ppb	25 ppb
H ₂	100 ppm [27]	1000 ppm [14]	–	10 ppm

such as O₂ or NO₂ comes in contact with SnO₂ surface, an electron-depleted space charge layer (as SnO₂ is an n-type semiconductor) is formed at the surface of SnO₂. This results in extraction of electrons from the SnO₂–SWNT interface resulting an increase in device conductivity. Similarly a reducing agent like NH₃ or H₂ will donate electrons hence decreasing device conductivity. The above explanation is consistent with our dynamic sensing experiments performed with different reducing and oxidizing gases.

Fig. 5a shows the sensor performance (reported as the percentage change in resistance, $\Delta R/R_0$ where R_0 is the baseline resistance) toward different concentrations of ammonia in dry air at 25 °C. The optimal electrical resistance of the sensors at room temperature was determined to be in the range of 10–100 kΩ, consistent with our previous work [22]. The SnO₂ nanoparticles decorated SWNT (with a deposition charge of 5 μC) showed greater response ($\Delta R/R_0$ of ~20% for 2.5 ppm_v of NH₃) compared to unfunctionalized SWNTs ($\Delta R/R_0$ of ~3% for 2.5 ppm_v of NH₃, center trace) or SWNTs completely encapsulated with SnO₂ (i.e., SnO₂–SWNTs with the deposition charge of 500 μC, bottom trace). In fact, a negative response is observed from the nanostructures ($\Delta R/R_0$ of ~–5% for 2.5 ppm_v of NH₃), which is consistent with FET measurements. Additionally, SnO₂–SWNT with a deposition charge of 5 μC was able to detect trace amount of H₂ (~10 ppm_v) and NO₂ (~25 ppb_v) whereas unfunctionalized SWNTs were insensitive toward these gases at such low concentrations (Fig. 5b and c). Similar observations were also observed toward H₂S, acetone, and water vapor (Fig. 5d–f). Furthermore, the sensing responses of control samples (i.e., SWNTs which underwent electrochemical treatment procedures without tin precursor) show similar response to unfunctionalized SWNTs (data not shown) indicating that SnO₂ nanoparticles on SWNTs greatly enhance the sensing performance.

The differences observed between the responses of SnO₂–SWNT hybrid nanostructures and unfunctionalized SWNT networks was expected since the concentration of oxygen defects and available surface area of active elements on SnO₂–SWNT hybrid structure are much greater than in unfunctionalized SWNTs. From TEM observations, it is clear that the SWNTs are coated with tin oxide nanoparticles with diameter ranging from 3 to 8 nm, resulting in an important increase in surface area for gas molecules interaction. Thus the greater sensitivity of SnO₂ coated SWNTs may be attributed to the high surface active elements (SnO₂) present on the surface of SWNTs facilitating both adsorption and charge transfer.

For chemical sensor characterization, two important parameters are considered: (1) change in resistance and (2) lowest limit of detection (i.e. concentration for a signal to noise ratio of 3). At least 5-fold changes in resistance are observed for SnO₂ coated SWNTs samples in comparison to unfunctionalized SWNTs (Fig. S2). Table 1 gives a comparison of limit of detection (LOD) for different analytes for SnO₂ nanowire sensor, SnO₂ coated multi-walled carbon nanotube (MWNT) hybrid networks, unfunctionalized SWNTs and SnO₂ coated SWNTs used in this study.

In earlier attempts by others, sensors made with tin oxide nanostructures only exhibited high sensitivity to trace amount of gases at temperatures typically exceeding 100 °C [24–26]. Recently, Huang et al. [27] fabricated a single SnO₂ nanorod sensor and were able to detect H₂ at concentration as low as 100 ppm_v at room temperature. Yang and coworkers [9] used SnO₂ nanostructures

to detect 3 ppm_v NO₂ at room temperature under UV illumination. For SnO₂–MWNT hybrid structures, room temperature sensing was observed, however the limit of detection was at least one order of magnitude higher than our results [14].

In summary, we have demonstrated a simple, controllable electrochemical approach to functionalize SnO₂ on SWNTs which shows promising applications toward room temperature gas sensing. High sensitivity may be attributed to (1) the greater availability of active surface sites for interactions and (2) nano p–n junctions on molecular interactions, whose depletion width can be effectively modulated by the subtle changes in the surrounding gaseous environment.

Supporting information

Optical image of sensor chip, high magnification SEM images, sensor performance toward NH₃, NO₂, H₂, H₂S, acetone, and water vapor.

Acknowledgments

Funding for the project was provided by the Defense Microelectronic Activity (DMEA) under agreement number H94003-05-2-0505 and the NIH Gene Environment Initiative through award U01 ES 016026.

Appendix A. Supplementary data

Supplementary data associated with this article can be found, in the online version, at <http://dx.doi.org/10.1016/j.electacta.2013.01.029>.

References

- [1] J. Janata, *Principles of Chemical Sensors*, Plenum, New York, 1989, p. 213.
- [2] R. Taylor, F.J.S. Schultz, *Handbook of Chemical and Biological Sensors*, IOP, Bristol and Philadelphia, 1996, p. 371.
- [3] N. Barsan, U. Weimar, Conduction model of metal oxide gas sensors, *Journal of Electroceramics* 7 (3) (2001) 143.
- [4] D. Kohl, Function and applications of gas sensors, *Journal of Physics D: Applied Physics* 34 (19) (2001) R125.
- [5] T. Sahn, L. Mädler, A. Gurlo, N. Barsan, S.E. Pratsinis, U. Weimar, Flame spray synthesis of tin dioxide nanoparticles for gas sensing, *Sensors and Actuators B: Chemical* 98 (2–3) (2004) 148.
- [6] M.H. Huang, S. Mao, H. Feick, H. Yan, Y. Wu, H. Kind, E. Weber, R. Russo, P. Yang, Room-temperature ultraviolet nanowire nanolasers, *Science* 292 (5523) (2001) 1897.
- [7] Z.W. Pan, Z.R. Dai, Z.L. Wang, Nanobelts of semiconducting oxides, *Science* 291 (5510) (2001) 1947.
- [8] M. Lai, J.-H. Lim, S. Mubeen, Y. Rheem, A. Mulchandani, M.A. Deshusses, N.V. Myung, Size-controlled electrochemical synthesis and properties of SnO₂ nanotubes, *Nanotechnology* 20 (18) (2009) 185602.
- [9] L. Matt, K. Hannes, M. Benjamin, K. Franklin, Y. Peidong, Photochemical sensing of NO₂ with SnO₂ nanoribbon nanosensors at room temperature, *Angewandte Chemie International Edition* 41 (13) (2002) 2405.
- [10] Y. Zhang, A. Kolmakov, S. Chretien, H. Metiu, M. Moskovits, Control of catalytic reactions at the surface of a metal oxide nanowire by manipulating electron density inside it, *Nano Letters* 4 (3) (2004) 403.
- [11] A. Kolmakov, D.O. Klenov, Y. Lilach, S. Stemmer, M. Moskovits, Enhanced gas sensing by individual SnO₂ nanowires and nanobelts functionalized with Pd catalyst particles, *Nano Letters* 5 (4) (2005) 667.
- [12] V.V. Sysoev, J. Goschnick, T. Schneider, E. Strelcov, A. Kolmakov, A gradient microarray electronic nose based on percolating SnO₂ nanowire sensing elements, *Nano Letters* 7 (10) (2007) 3182.

- [13] C. Yu, Q. Hao, S. Saha, L. Shi, X. Kong, Z.L. Wang, Integration of metal oxide nanobelts with microsystems for nerve agent detection, *Applied Physics Letters* 86 (6) (2005) 063101.
- [14] G.H. Lu, L.E. Ocola, J.H. Chen, Room-temperature gas sensing based on electron transfer between discrete tin oxide nanocrystals and multiwalled carbon nanotubes, *Advanced Materials* 21 (24) (2009) 2487.
- [15] Z. Wen, Q. Wang, Q. Zhang, J. Li, *In situ* growth of mesoporous SnO₂ on multiwalled carbon nanotubes: a novel composite with porous-tube structure as anode for lithium batteries, *Advanced Functional Materials* 17 (15) (2007) 2772.
- [16] A. Yang, X. Tao, R. Wang, S. Lee, C. Surya, Room temperature gas sensing properties of SnO₂/multiwall-carbon-nanotube composite nanofibers, *Applied Physics Letters* 91 (13) (2007) 133110.
- [17] W.-Q. Han, A. Zettl, Coating single-walled carbon nanotubes with tin oxide, *Nano Letters* 3 (5) (2003) 681.
- [18] L. Zhao, M. Choi, H.-S. Kim, S.-H. Hong, The effect of multiwalled carbon nanotube doping on the CO gas sensitivity of SnO₂-based nanomaterials, *Nanotechnology* 18 (44) (2007) 445501.
- [19] Z. Miao, D. Xu, J. Ouyang, G. Guo, X. Zhao, Y. Tang, Electrochemically induced sol gel preparation of single-crystalline TiO₂ nanowires, *Nano Letters* 2 (7) (2002) 717.
- [20] A. Walcarius, E. Sibottier, M. Etienne, J. Ghanbaja, Electrochemically assisted self-assembly of mesoporous silica thin films, *Nature Materials* 6 (8) (2007) 602.
- [21] J.H. Lim, N. Phiboolsirichit, S. Mubeen, Y.W. Rheem, M.A. Deshusses, A. Mulchandani, N.V. Myung, Electron and sensing properties of single-walled carbon nanotubes network: effect of the alignment and selective breakdown, *Electroanalysis* 22 (1) (2010) 99.
- [22] S. Mubeen, T. Zhang, B. Yoo, M.A. Deshusses, N.V. Myung, Palladium nanoparticles decorated single-walled carbon nanotube hydrogen sensor, *Journal of Physical Chemistry C* 111 (17) (2007) 6321.
- [23] S.J. Tans, A.R.M. Verschueren, C. Dekker, Room-temperature transistor based on a single carbon nanotube, *Nature* 393 (6680) (1998) 49.
- [24] C. Baratto, E. Comini, G. Faglia, G. Sberveglieri, M. Zha, A. Zappettini, Metal oxide nanocrystals for gas sensing, *Sensors and Actuators B: Chemical* 109 (1) (2005) 2.
- [25] E. Comini, G. Faglia, G. Sberveglieri, Z. Pan, Z.L. Wang, Stable and highly sensitive gas sensors based on semiconducting oxide nanobelts, *Applied Physics Letters* 81 (10) (2002) 1869.
- [26] H. Huang, Y.C. Lee, C.L. Chow, O.K. Tan, M.S. Tse, J. Guo, T. White, Plasma treatment of SnO₂ nanocolumn arrays deposited by liquid injection plasma-enhanced chemical vapor deposition for gas sensors, *Sensors and Actuators B: Chemical* 138 (1) (2009) 201.
- [27] H. Huang, Y.C. Lee, O.K. Tan, W. Zhou, N. Peng, Q. Zhang, High sensitivity SnO₂ single-nanorod sensors for the detection of H₂ gas at low temperature, *Nanotechnology* 20 (11) (2009) 115501.